ANNALI DI GEOFISICA, VOL. XXXVII, N. 3, June 1994

Preliminary calibration of candidate alpha stations in the GSETT-3 network

Hans-Peter Harjes, Michael Jost and Johannes Schweitzer
Institute of Geophysics, Ruhr-University, Bochum, Germany

Abstract
The technical concept of a future global seismic monitoring system includes 50 to 60 core stations, mostly arrays, which provide the primary detection and location capability. Due to the average station distance, these core («alpha») stations form a teleseismic network. Many of the proposed stations are to be newly installed and before the network can be regarded as fully operational, the stations have to be calibrated. As for traditional seismic networks, the station residuals – compared to a standard earth model – have to be determined. The standard earth model is defined in terms of travel-time tables and amplitude-distance curves. After recording a representative set of events, station residuals with respect to travel-time and magnitude can be calculated. In case of arrays, the determination of mislocation vectors (azimuth and slowness residuals) are of utmost importance if array slowness vectors are used as starting solutions in a location procedure. Finally, in a monitoring context it is very important to estimate the station sensitivity for varying background noise conditions and – in case of arrays – to know the frequency dependent improvement by beamforming. This paper uses the newly installed high-frequency GERESS array in Germany to demonstrate the calibration procedure.

Key words *global seismic networks – station calibration – array location – magnitude residuals*

1. Introduction

The Group of Scientific Experts (GSE) is currently developing a final concept for an international seismic data exchange system which includes a three-tiered global network of stations where the first tier, the so-called alpha-network, consists primarily of arrays, with some three-component stations, and is designed to provide not only the required detection threshold throughout the world but also to achieve a preliminary event location which is then improved by the supplementary beta and gamma networks.

In contrast to the station network used during the previous test (GSETT-2) which may more appropriately be called an arbitrary collection of stations, the alpha stations for GSETT-3 are carefully chosen from the latest and most modern installations taking into account a uniform global coverage. To form a true network, the alpha stations have to be calibrated. This calibration includes characterization of the station noise, an estimate of station sensitivity, signal to noise ratio improvement by beamforming (in case of arrays), the station residuals w.r.t. travel-time and magnitude, and the determination of mislocation vectors.

In the following paragraphs some elements of the calibration procedure are described using the GERESS array as an example for an alpha station. Whereas the complete GSETT-3 network calibration can

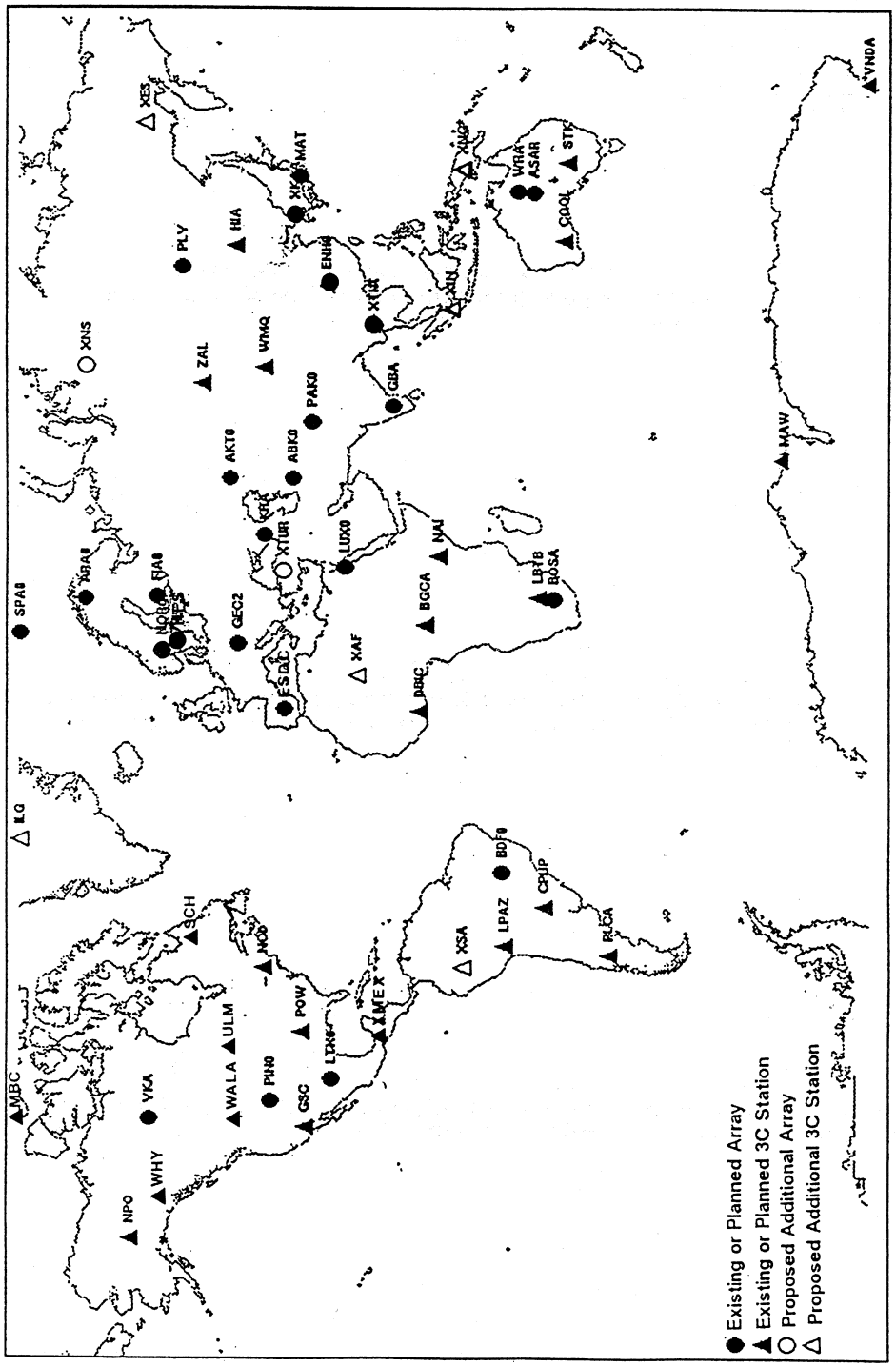

Fig. 1. Preliminary GSETT-3 alpha network. The filled symbols represent existing or planned stations. The open symbols denote additional stations that are proposed to be located in certain general geographical regions so as to improve the global coverage. The additional stations could be chosen either from existing stations or by installation of new facilities.

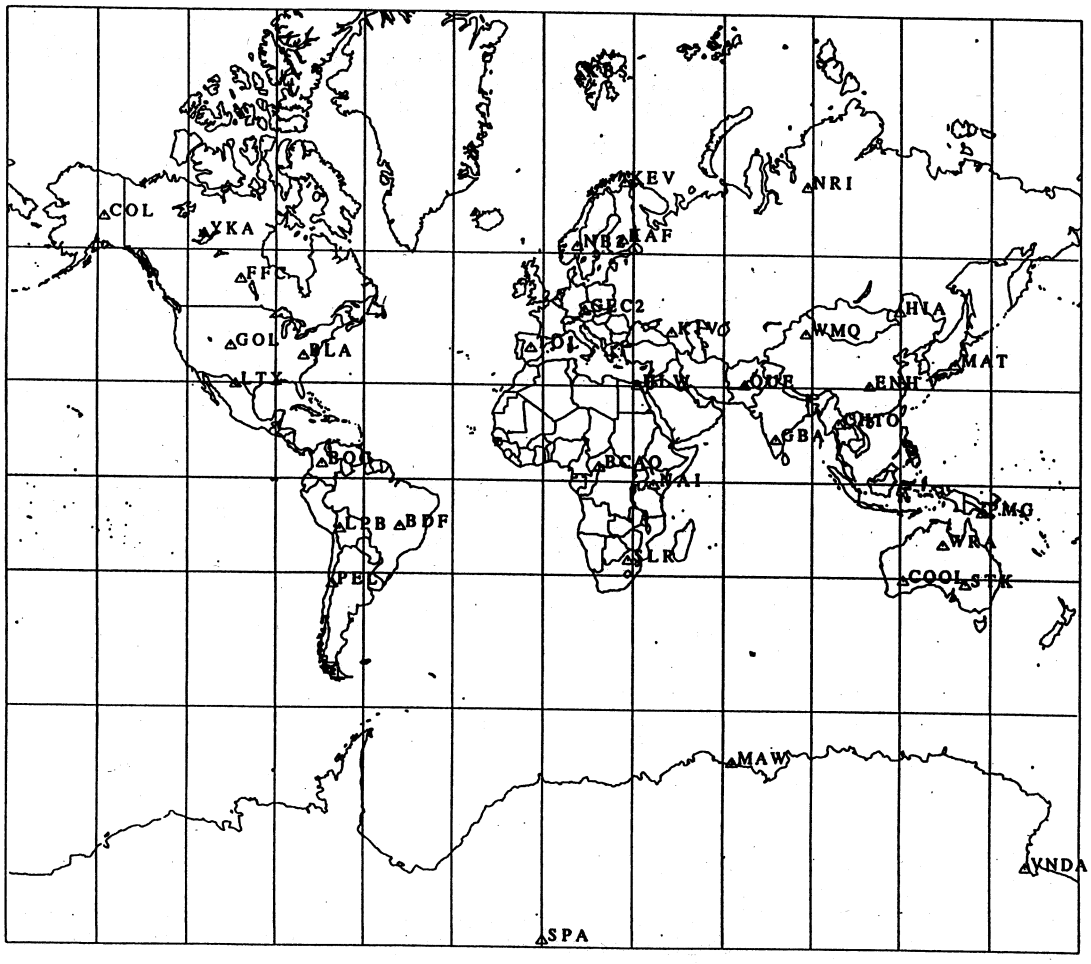

Fig. 2. Substitute NEIC-network used in this study.

only be performed after the system has been operational for a significant time period, the method can be explained by using existing stations which reported to the US National Earthquake Information Center (NEIC) in the past. In this way, 36 stations were selected which are either part of the proposed alpha network or which are closely located to a proposed alpha station.

Figure 1 shows the configuration of the GSETT-3 alpha network which includes 26 arrays and 28 single-site stations. In comparison, the network used in this study (fig. 2) contains 6 arrays and 30 single-site stations.

2. Station noise characteristics

The capability of a seismic station to detect a signal across the frequency bandwidth of its sensor is limited by the effective noise measured at these frequencies.

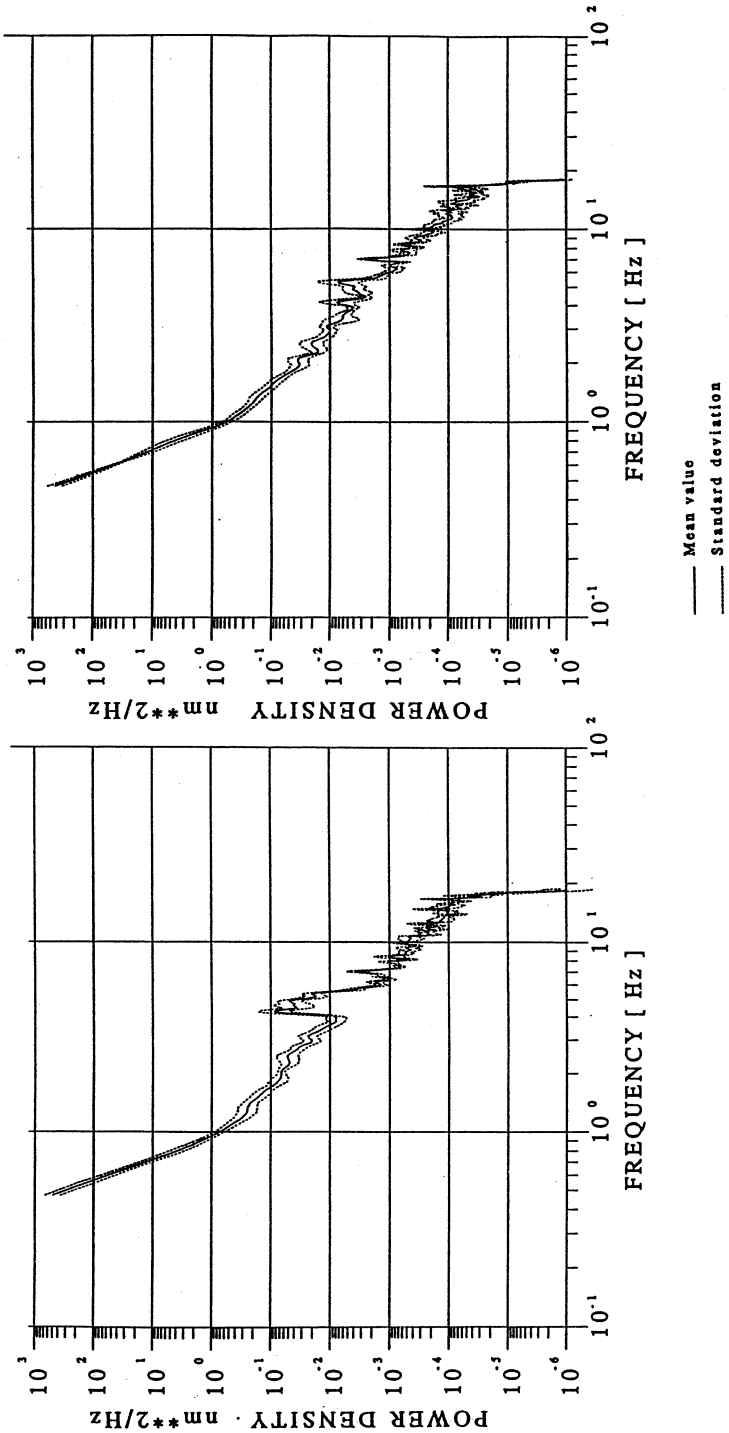

Fig. 3. Short-period vertical component displacement power spectrum at the key-station GEC2 for day time (left) and night time (right).

The large data base of seismic waveforms collected during GSETT-2 offered the first opportunity for a quantitative analysis of noise conditions. Across the GSETT 2 network, noise amplitudes varied by more than a factor of 10 around 1 Hz – the frequency range which is most important for teleseismic detection. The temporal variation of noise conditions has a significant influence on the station's detection performance. As an example, fig. 3 shows the noise spectrum for GERESS measured at day time (left) and night time (right). The noise level at daylight time is increased as a result of human and industrial (mining) activities. As a consequence of the higher noise level during daylight hours, the detection probability is decreased by about 8% compared to night time. Figure 4 shows the same effect for a different station (KHC) which is located on the same geological unit (Bohemian massif) as GERESS. This similarity confirms that the daily variation is not a local singularity at GERESS but a common feature for seismic stations in industrialized areas as Central Europe.

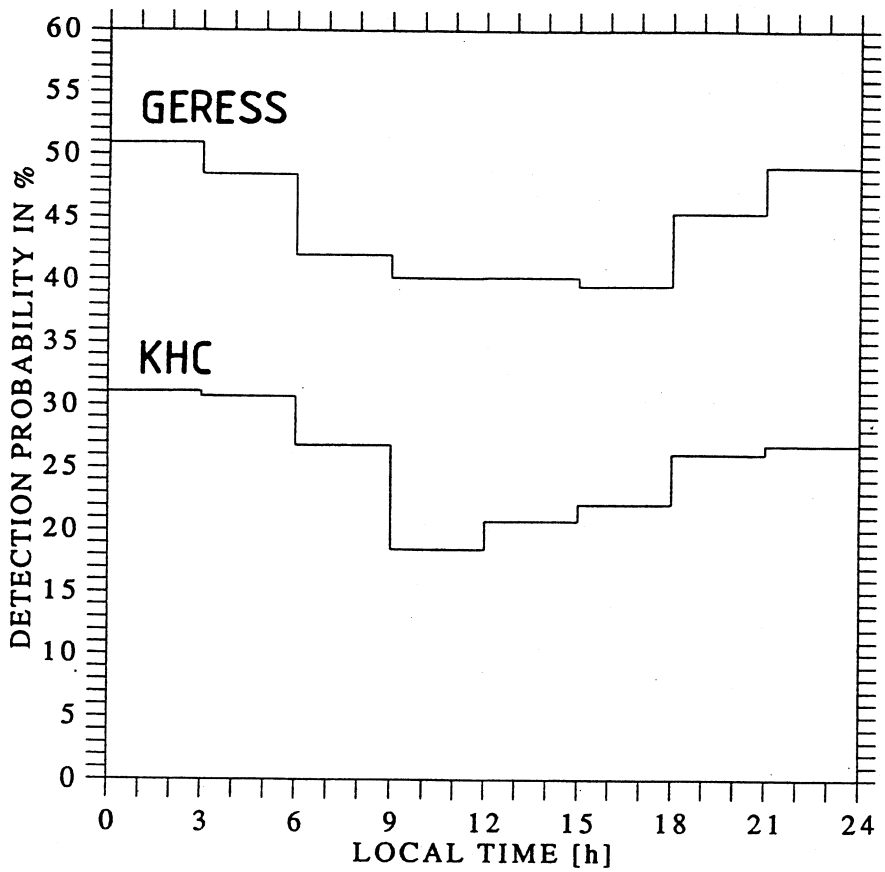

Fig. 4. Detection probability for teleseismic events ($\Delta > 20^{o}$) as a function of time of day for GERESS (upper line) and KHC (lower line).

Whereas the time period of GSETT-2 was not long enough to reveal seasonal noise variation, our study shows remarkable differences. As an example, fig. 5 compares the detection capability of GERESS with the Yellowknife array (YKA) for a time period of 16 months. YKA shows a decrease of about 25% during summer when the Great Slave Lake – located close to YKA – is open. There appears very little seasonal variation at GERESS.

From this result it can be concluded that the GSETT-3 alpha network needs to be operated at least one year to understand the detection performance and to estimate its temporal variation.

3. Station sensitivity

The detection capability of a station is not only influenced by the local noise conditions but also by the site response; *i.e.* the signal amplification due to the receiver crust. As a consequence, the station sensitivity varies with frequency and station-specific passbands are used for automatic signal detectors. In addition, the signal-to-noise improvement achievable by arrays is frequency dependent and cannot simply be estimated from the $\sqrt{(N)}$ -rule (N-number of sensors). In the past, P-wave detectability studies have been performed for only few arrays like NORESS (Kværna, 1989). A similar study was undertaken for GERESS (Jost, 1992). Figure 6 shows a comparison for both arrays which is based on 25 channels at NORESS (14 db) and 22 channels at GERESS (13.4 db). GERESS shows a higher P-wave detectability in the teleseismic frequency range 1-3 Hz, while NORESS is superior for higher frequencies which are important for the detection of regional phases. The differencies between GERESS and NORESS can be partly explained by the noise characteristics at both arrays.

As arrays are the «backbone» of the

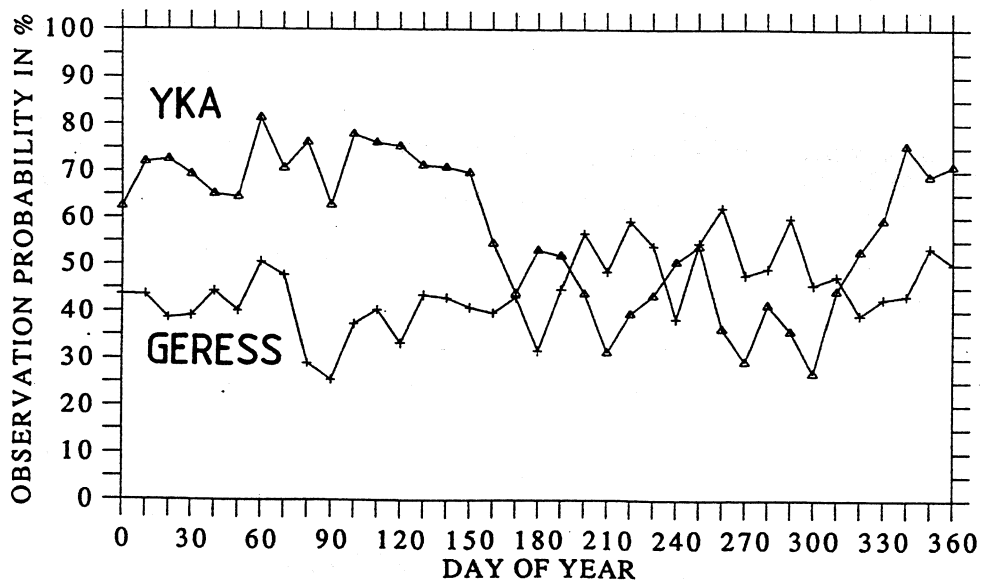

Fig. 5. Seasonal variation of teleseismic ($\Delta > 20^{\circ}$) detection probability for GERESS and YKA (October 18, 1991 – February 11, 1993).

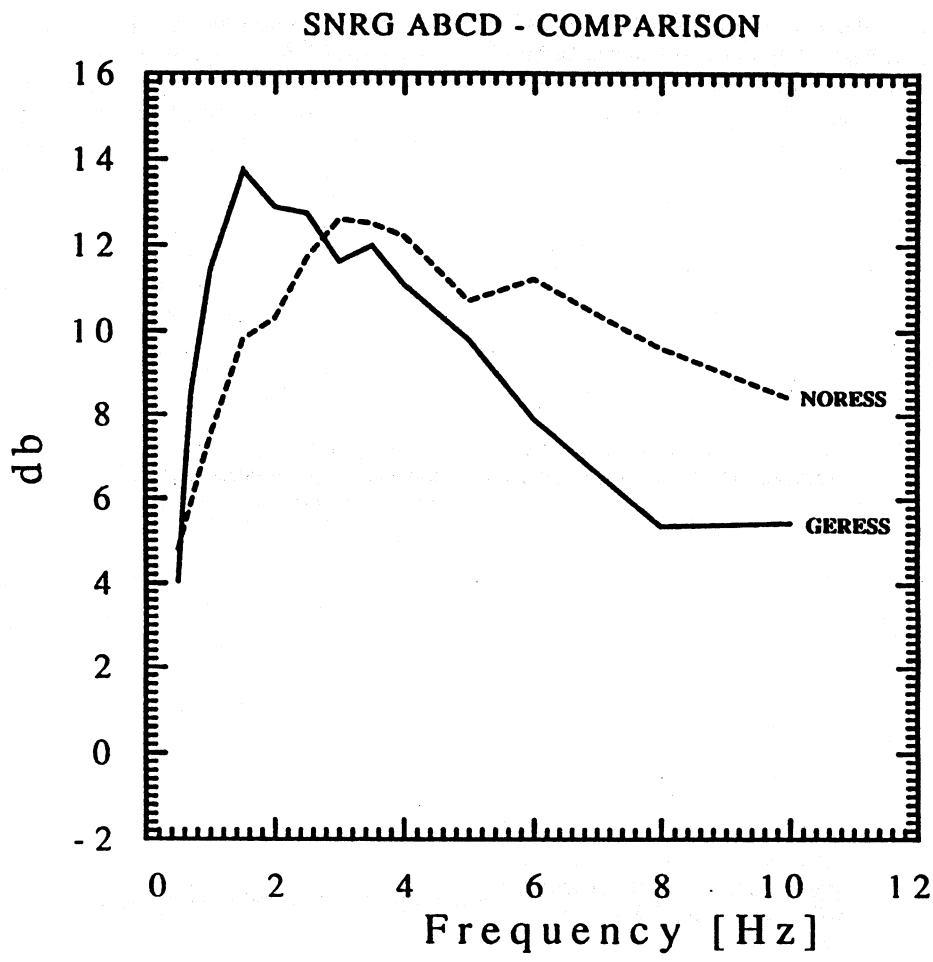

Fig. 6. Mean curves of SNR-gain for GERESS and NORESS.

GSETT-3 alpha network, a similar investigation is needed for all arrays within the alpha network to optimize the detection capability. A representative set of strong local, regional, and teleseismic signals must be recorded before such a study can be undertaken.

4. Travel time and amplitude residuals

Compared to the large number of stations (about 1500) reporting to NEIC, the GSETT-3 alpha network of 52 stations is still to be regarded as a sparse station distribution. Especially at the detection threshold only few stations will contribute to an event formation. Station calibration with respect to travel time and signal amplitude is therefore of utmost importance. In a separate investigation (Schweitzer, 1993), we have determined the travel time residuals for the network described above (fig. 2) using only large and well constrained events (m_b > 5.0 (NEIC), more than 19 defining P phases). In addition, onsets with

an absolute value of the travel time residual larger than 3.0 s were rejected. The mean travel time residuals of first arrivals (*P* or *PKP*) for all stations are summarized in table I. Taking GERESS as an example, the residual based on 1520 phases is −0.66 s with a standard deviation of ± 0.68 s. Figure 7 shows the mean travel time residuals of all stations.

Residuals are plotted with respect to the percentage of observed Earthquake Data Report (EDR) events. The comparison is based on the contribution of seismic stations from April 1990 to June 10, 1993. The percentage of observed events gives a rough idea of the sensitivity of the stations. It is obvious that all highly sensitive arrays have negative travel time residuals and that single stations show a similar trend: the more sensitive the station, the more negative is its travel time bias. This observation is confirmed by Grand (1990), who showed that the travel time residuals of different stations in the ISC bulletins correlate with the amplification of the stations. This result suggests that the source times of larger events can be systematically biased to later times due to a large number of less sensitive stations which observed these events.

For the estimation of the magnitude (amplitude) residuals, the same events as for the travel time analysis were used. Table I includes the resulting values for those stations which report amplitudes to NEIC. As an example GERESS contributed to 945 m_b values. The mean m_b residual at GERESS is −0.60 with a standard deviation of 0.35.

This relatively large magnitude residual results from several effects that all tend to decrease measured amplitudes: first, GERESS has its best SNR gain for *P* onsets in the frequency range between 1.0 Hz and 3.0 Hz (compare section 3). Therefore, this narrow frequency band is often used to measure amplitudes (note that many of

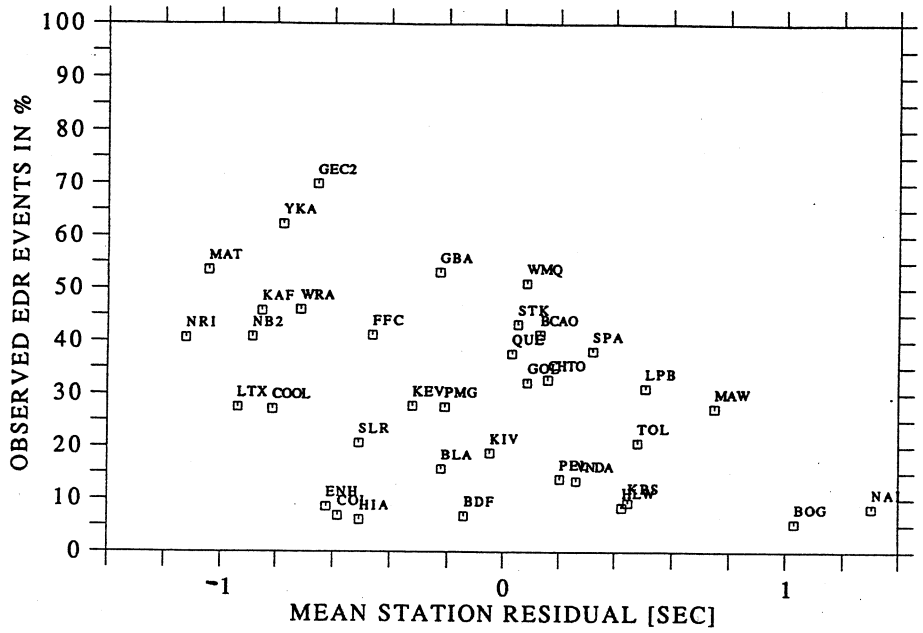

Fig. 7. Travel time residuals of stations from fig. 2 compared to percentage of observed NEIC-events.

Table I. Travel time and magnitude residuals for stations from fig. 2 (stations in brackets are substitutes for collocated alpha stations).

Station	Percentage of NEIC events	Travel time-residuals (s) (n. of reportings)	m_b Residuals (n. of reportings)
ABK0	–	–	–
AKT0	–	–	–
ARA0	–	–	–
(KEV)	27.7	−0.32 (1203)	−0.02 (497)
ASAR	–	–	–
BDFB	–	–	–
(BDF)	6.8	−0.14 (186)	–
BGCA	–	–	–
(BCAO)	41.2	0.13 (1255)	0.11 (570)
BOSA	–	–	–
(SLR)	20.7	−0.51 (909)	0.04 (432)
COOL	27.2	−0.81 (1195)	−0.23 (381)
CPUP	–	–	–
DBIC	–	–	–
ENH0	–	–	–
(ENH)	8.6	−0.62 (81)	–
ESLA	–	–	–
(TOL)	20.7	0.48 (778)	0.39 (264)
FFC	41.1	−0.46 (1144)	0.01 (991)
FIA0	–	–	–
(KAF)	45.7	−0.85 (1607)	−0.09 (1084)
GBA	53.0	−0.23 (1685)	−0.25 (767)
GEC2	69.8	−0.66 (1520)	−0.60 (945)
HIA	6.1	−0.51 (220)	–
ILG	–	–	–
KIV0	–	–	–
(KIV)	18.8	−0.05 (196)	–
LBTB	–	–	–
LPAZ	–	–	–
(LPB)	31.0	0.51 (1298)	0.33 (158)
LTX0	–	–	–
(LTX)	27.5	−0.94 (95)	–
LUX0	–	–	–
(HLW)	8.4	0.43 (345)	–
MAT	53.5	−1.04 (2083)	−0.16 (1583)
MAW	27.2	0.75 (1190)	−0.10 (665)
NAI	8.3	1.30 (345)	0.31 (79)

Table I. (*continued*) Travel time and magnitude residuals for stations from fig. 2 (stations in brackets are substitutes for collocated alpha stations).

Station	Percentage of NEIC events	Travel time-residuals (s) (n. of reportings)	m_b Residuals (n. of reportings)
MNQ	–	–	–
NOR0	–	–	–
(NB2)	40.8	−0.89 (1789)	−0.16 (1334)
NPO	–	–	–
(COL)	6.9	−0.58 (270)	–
NRI0	–	–	–
(NRI)	40.6	−1.12 (371)	−0.03 (277)
NVS	–	–	–
PAK0	–	–	–
(QUE)	37.6	0.03 (1599)	0.36 (213)
PIN0	–	–	–
(GOL)	32.1	0.09 (1401)	−0.22 (971)
PLCA	–	–	–
(PEL)	13.8	0.20 (546)	0.16 (131)
PLY	–	–	–
SPA	38.1	0.32 (1658)	0.06 (1422)
SPA0	–	–	–
(KBS)	9.2	0.45 (361)	–
STK	43.2	0.05 (1597)	−0.47 (1351)
VNDA	13.4	0.26 (71)	–
WMQ	50.9	0.08 (1929)	0.04 (973)
WRA	45.9	−0.72 (1815)	−0.30 (1343)
XAF	–	–	–
XES	–	–	–
XEUS	–	–	–
(BLA)	15.7	−0.22 (681)	−0.05 (471)
XIN	–	–	–
XKOR	–	–	–
XNG	–	–	–
(PMG)	27.6	−0.21 (1040)	0.22 (361)
XSA	–	–	–
(BOG)	5.4	1.03 (201)	–
XTIA	–	–	–
(CHTO)	32.7	0.16 (1233)	−0.27 (783)
XTUR	–	–	–
XWUS	–	–	–
YKA	62.2	−0.78 (2718)	−0.46 (2415)

these onsets would not be visible on a WWSSN short-period instrument at the GERESS site). This narrow-band filtering increases the SNR but decreases the mean amplitudes. Secondly, some signal loss can occur due to beamforming. Finally, at GERESS, we generally do not observe any site amplification due to the missing sedimentary cover. Figure 8 shows m_b residuals of all stations plotted with respect to the mean reported period T to compute $\log A/T$ (which is thought to compensate for different instrumentation and observing periods).

In conclusion, travel time and amplitude residuals influence the quality of event bulletins significantly. As a result of station-specific frequency filters used for improving the detection capability, travel times and amplitudes have to be corrected for phase response and bandwidth of the individual filters.

5. Mislocation vectors

In the new GSE-concept the alpha stations not only provide data to detect phases but these detections are also used to get a first estimate of the location of events. Very often, these location estimates will depend on data from very few stations and directional data (slowness and azimuth or angle of incidence) are essential in this location procedure. During GSETT-2, when directional data were used for the first time for epicentre determination, the accuracy of slowness-vector estimates varied enormously among stations. From this experience it was concluded that arrays and single-site stations need to be calibrated on an individual basis. In the following, this procedure will be demonstrated for the GERESS array again taking the NEIC bulletin as a reference.

Although the small aperture (4 km) GERESS array has only limited resolution

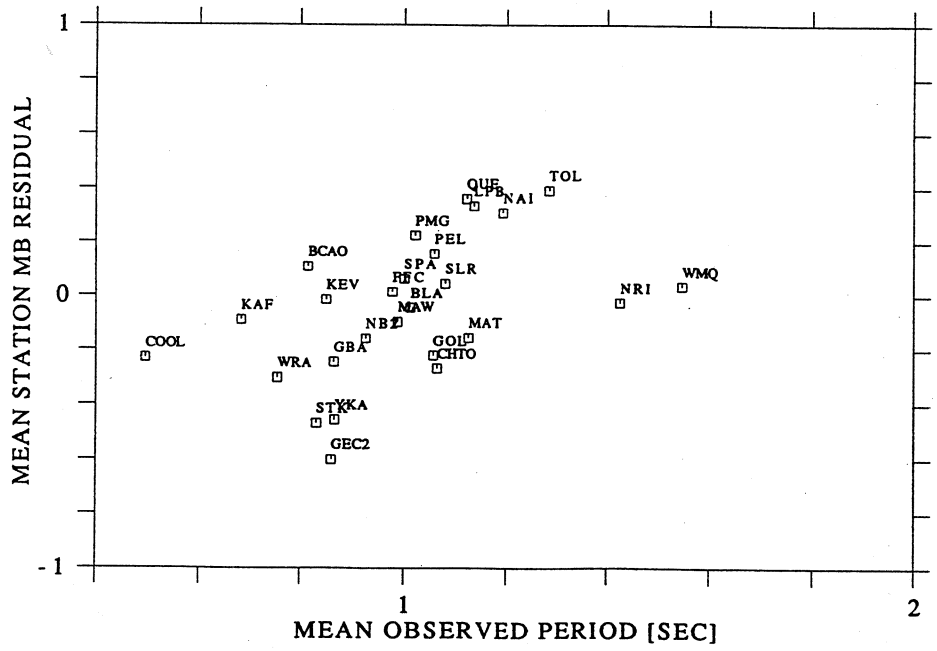

Fig. 8. Mean station m_b-residual as a function of mean observing period.

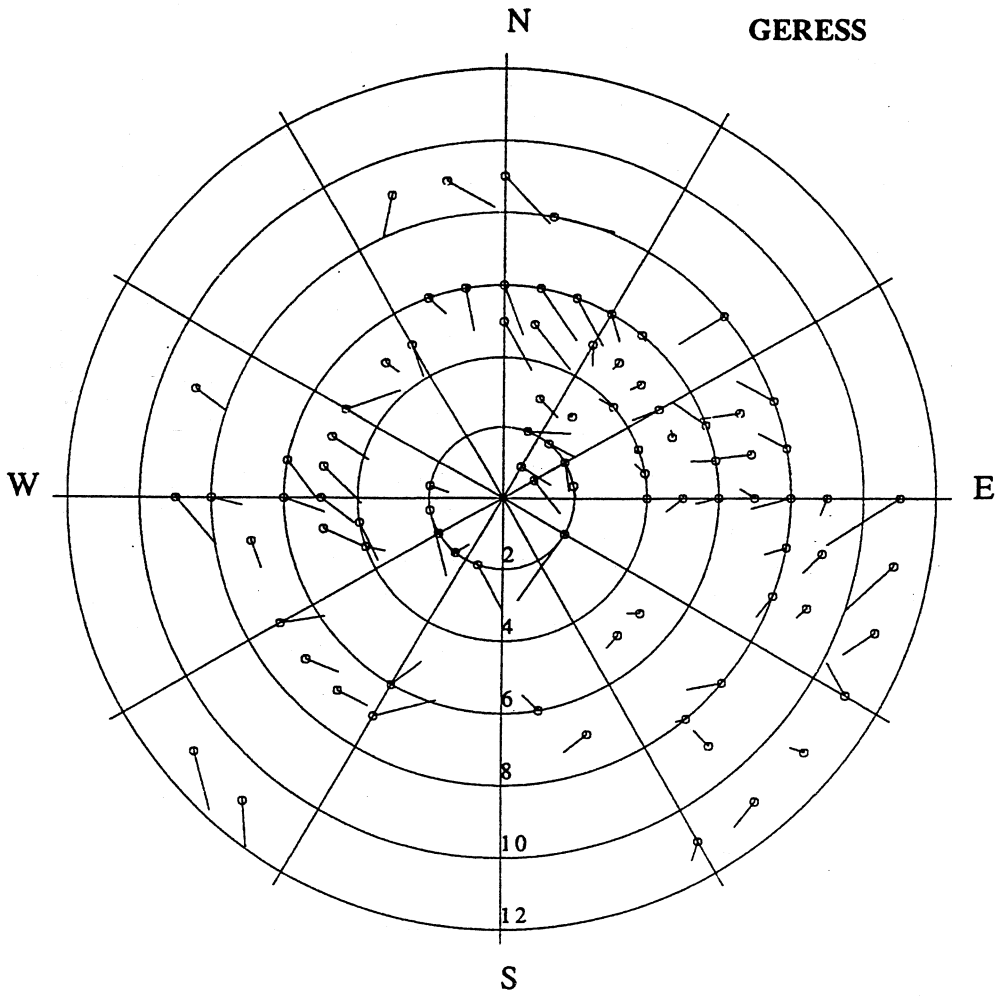

Fig. 9a. Mean mislocation vectors for GERESS calculated from at least 5 observations.

for measuring slowness and back-azimuth (BAZ) of teleseismic onsets, the differences to theoretical values have been determined. Locations of NEIC were used to calculate epicentral distance and theoretical BAZ; the IASP91 travel time tables (Kennett and Engdahl, 1991) were employed to calculate the theoretical slowness of the first arrival (*P*, *P*diff, *PKP*) using theoretical epicentral distance and reported depth (NEIC). All slowness and BAZ values of first arrivals with a travel time residual $| t_{obs} - t_{theo} | > 3.0$ s and with a slowness mislocation vector of more than 4.0 s/deg were omitted. With the first arrivals analysed during the GSETT-2 period and the phases reported between October 18, 1991 and June 10, 1993, a total of 3910 slowness and BAZ values were available.

Figure 9a shows the observed mislocation vectors in slowness space, which has been divided into cells (1 s/deg by 10 deg in

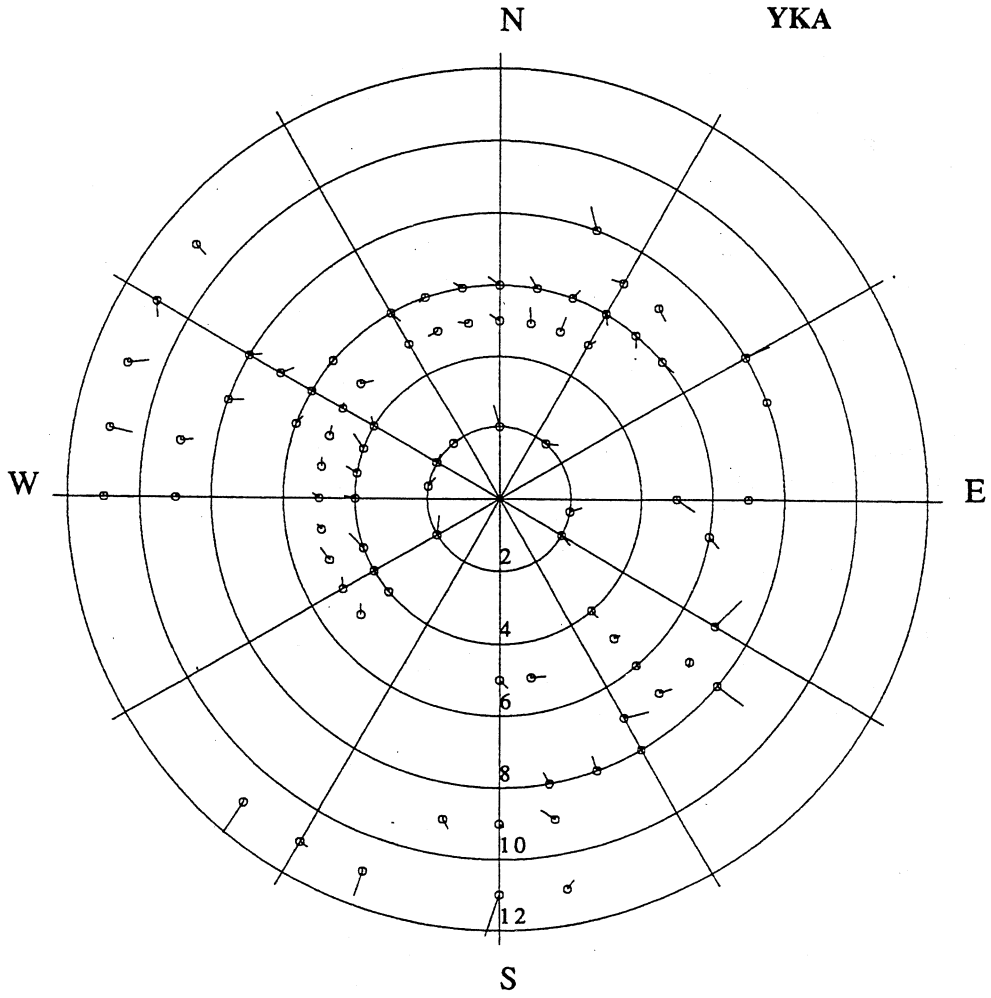

Fig. 9b. Mean mislocation vectors for YKA calculated from at least 5 observations.

the outer regions and 1 s/deg by 20-30 deg in the central part). Mislocation vectors displayed are averages for each cell in the slowness space and contain at least 5 observations. The theoretical value is indicated by a circle. The mean slowness residual of all observations is −0.42 s/deg with a standard deviation of 1.17 s/deg. The mean BAZ residual is 5.3 deg with a standard deviation of 23.7 deg. The figure shows that BAZ residuals have a common trend: they change from positive residuals between 350 deg. to 30 deg and from 90 deg to 170 deg to negative residuals from 40 deg to 80 deg and from 180 deg to 340 deg. The observed slowness values are systematically too small with respect to IASP91. It remains to be analysed, whether this observation is due to the Earth's structure, the local geology, the topography at the array site, the array configuration, or just the algorithm of the implemented *fk*-analysis. Most of the misloca-

tion vectors of GERESS in fig. 9a are small with respect to their standard deviation. Therefore it may not be useful, to correct the observed slowness and BAZ values with above mislocation vectors. Until a more complete set of mislocation vectors becomes available, mean standard deviations (1.17 s/deg and 23.7 deg) can be used to weight the GERESS slowness and BAZ values in location algorithms (*e.g.*, the Intelligent Monitoring System, IMS).

Since January 1992, YKA and GERESS have been regularly exchanging their phase readings via electronic mail. Therefore slowness and azimuth values reported from YKA can be compared with theoretical values using again NEIC locations. Figure 9b shows the YKA mislocation vectors for 3679 phases for the time period from January 6, 1992 to February 18 1993. The mean slowness error of YKA is 0.02 s/deg with a standard deviation of 0.46 s/deg and the mean back-azimuth error is 0.61 deg with a standard deviation of 5.31 deg. The array aperture of YKA is larger than GERESS and this difference yields a better resolution for YKA.

6. Conclusions

For calibrating an alpha station, various investigations are recommended: the characterization of the noise, the estimation of the station sensitivity as a function of frequency (including signal to noise ratio improvement by beamforming for arrays), and the determination of station residuals (w.r.t. travel-time, slowness vector, and magnitude).

In this paper, some calibration parameters are preliminary estimated for some alpha stations which reported to NEIC in the past. This study intends to demonstrate the method and importance of calibration of a network in order to produce a high-quality bulletin. It has been mentioned that a calibration of the GSETT-3 alpha network can only be conducted after that network operated for a sufficient time period (*i.e.* at least one year).

REFERENCES

GRAND, S.P. (1990): A possible station bias in travel time measurements reported to ISC, *Geophy. Res. Let.*, **17**, 17-20.

JOST, M. (1992): GERESS *P*-wave detectability, in *Advanced Waveform Research Methods for GERESS Recordings*, ARPA Annual Report N. AFOSR-90-0189, Scientific Report N. 2, PL-TR-92-2142, 13-24.

KENNETT, B.L.N. and E.R. ENGDAHL (1991): Travel times for global earthquake location and phase identification, *Geophys. J. Int.*, **105**, 429-466.

KVÆRNA, T. (1989): On exploitation of small-aperture NORESS type arrays for enhanced *P*-wave detectability, *Bull. Seismol. Soc. Am.*, **79**, 888-900.

SCHWEITZER, J. (1993): Teleseismic detection and location capabilities of the GERESS array, in *Advanced Waveform Research Methods for GERESS Recordings*, ARPA Annual Report N. AFOSR-90-0189, Scientific Report N. 3, 33-50.